Vs-Based Evaluation of Select Liquefaction Case Histories from the 2010–2011 Canterbury Earthquake Sequence

Clinton M. Wood, A.M.ASCE¹; Brady R. Cox, A.M.ASCE²; Russell A. Green, A.M.ASCE³; Liam M. Wotherspoon⁴; Brendon A. Bradley⁵; and Misko Cubrinovski⁶

Abstract: The 2010–2011 Canterbury earthquake sequence included a number of events that triggered recurrent soil liquefaction at many locations in Christchurch, New Zealand. However, the most severe liquefaction was induced by the M_w 7.1 September 4, 2010, Darfield and M_w 6.2 February 22, 2011, Christchurch earthquakes. The combination of well-documented liquefaction surface manifestations during multiple events, densely recorded ground motions during these events, and detailed subsurface characterization information at the selected sites provides an unprecedented opportunity to add quality case histories to the empirical soil liquefaction database. The authors have already documented and published 50 high-quality liquefaction case histories from these earthquakes using cone penetration test (CPT) data. This paper examines 46 of these case histories using shear-wave velocity (Vs) profiles derived from surface wave (SW) methods and a Christchurch-specific Vs correlation based on CPT tip resistance. The Vs profiles have been used to evaluate the two most commonly used Vs-based simplified liquefaction evaluation procedures (i.e., Andrus and Stokoe and Kayen et al.). An error index (E_I) has been used to quantify the overall performance of these two procedures in relation to liquefaction observations. Although the two procedures are essentially equivalent for sites with normalized Vs (i.e., Vs1) <180 m/s, the Kayen et al. procedure, with 15% probability of liquefaction, provides better predictions of liquefaction triggering for sites with Vs1 greater than 180 m/s. Additionally, total E_I values obtained using Vs profiles from surface wave testing in conjunction with the Kayen et al. procedure are lower than two other CPT-based triggering procedures but higher than the total E_I value obtained using the Idriss and Boulanger CPT-based procedure. **DOI:** 10.1061/(ASCE)GT.1943-5606.0001754. © 2017 American Society of Civil Engineers.

Introduction

The 2010–2011 Canterbury earthquake sequence (CES) comprised up to 10 events that triggered liquefaction in the greater Christchurch, New Zealand, region (Quigley et al. 2013). The CES provided a unique opportunity to add numerous high-quality liquefaction case histories to existing databases because of the dense network of strong motion stations (SMSs), the well-documented observations of liquefaction surface manifestations, and the detailed subsurface characterization performed at many sites (Cousins and McVerry 2010; Bradley and Cubrinovski 2011; Bradley 2012a, b). For example, Green et al. (2014) documented 25 case history sites resulting from observations of liquefaction following both the September 4, 2010, M_w 7.1 Darfield and

Note. This manuscript was submitted on July 15, 2016; approved on March 21, 2017; published online on June 26, 2017. Discussion period open until November 26, 2017; separate discussions must be submitted for individual papers. This paper is part of the *Journal of Geotechnical and Geoenvironmental Engineering*, © ASCE, ISSN 1090-0241.

February 22, 2011, M_w 6.2 Christchurch earthquakes (25 case history sites with ground motions and liquefaction observations from two different earthquakes equals 50 distinct case history data points). The case history sites selected by Green et al. (2014) were chosen based on proximity to strong motion stations and observations of liquefaction response during both earthquakes, with the goal of selecting sites exhibiting either minor or no liquefaction in one event and minor to severe liquefaction in the other event. This approach to case history selection was aimed at more accurately evaluating the position of the cyclic resistance ratio (CRR) curve because each site had a case history data point on each "side" of or near the triggering curve. Green et al. (2014) used data collected at these 25 sites to evaluate three common CPT-based liquefaction triggering relationships using a quantitative error index. In this paper, 23 of the original case history sites are used to evaluate two existing shear wave velocity-based simplified liquefaction triggering procedures using the same error index.

The use of shear-wave velocity (Vs) to evaluate liquefaction triggering is often overshadowed by more widely used in situ penetration tests such as the standard penetration test (SPT) and the cone penetration test (CPT). Greater familiarity with the SPT and CPT methods, along with their extensive databases of liquefaction case histories, contributes significantly to their preferential use over Vs. Furthermore, SPT and CPT are strongly influenced by soil density, which is one of the key factors affecting liquefaction susceptibility. However, subtle yet potentially important, changes in density may not be accompanied by significant changes in Vs (Idriss and Boulanger 2008). Nonetheless, Vs has some distinct advantages over in situ penetration tests, the most basic being that Vs can be used to directly calculate the small-strain shear modulus (a fundamental soil property) and can be measured in both the lab and the field using a number of methods. Furthermore, Vs is more sensitive to the effects of aging, preshaking, cementation, and soil

¹Assistant Professor, Dept. of Civil Engineering, Univ. of Arkansas, 4190 Bell Engineering Center, Fayetteville, AR 72701 (corresponding author). E-mail: cmwood@uark.edu

²Associate Professor, Dept. of Civil, Architectural, and Environmental Engineering, Univ. of Texas at Austin, 301 E. Dean Keeton St., Austin, TX 78712.

³Professor, Dept. of Civil and Environmental Engineering, Virginia Tech, 200 Patton Hall, Blacksburg, VA 24061.

⁴Senior Lecturer, Dept. of Civil and Environmental Engineering, Univ. of Auckland, Private Bag 92019, Auckland 1142, New Zealand.

⁵Professor, Dept. of Civil and Natural Resources Engineering, Univ. of Canterbury, Private Bag 4800, Christchurch 8140, New Zealand.

⁶Professor, Dept. of Civil and Natural Resources Engineering, Univ. of Canterbury, Private Bag 4800, Christchurch 8140, New Zealand.

microstructure than penetration testing, and these factors can play an important role in understanding liquefaction triggering (El-Sekelly et al. 2015). Also, Vs is considerably less sensitive to the influence of soil fines content in comparison with SPT and CPT (Kayen et al. 2013). Thus, Vs and penetration testing complement one another, and their combined use to more fully understand liquefaction susceptibility is becoming more regularly encouraged (Robertson 2015; Schneider and Moss 2011). Hence, it is important to understand which Vs-based liquefaction triggering relationships are best suited for predicting liquefaction susceptibility.

In this paper, Vs profiles collected at 23 case history sites are used to evaluate the Vs-based simplified liquefaction evaluation procedures proposed by Andrus and Stokoe (2000) and Kayen et al. (2013). The liquefaction procedures are assessed by comparing the predicted factors of safety against liquefaction with observed surficial manifestation at each site. The liquefaction surficial manifestations at each site were determined by Green et al. (2014) using one or more of these three methods: (1) immediate postearthquake site visits by the authors, (2) examination of high-resolution aerial and satellite imagery, and/or (3) interviews with residents who lived near the case history sites. Each Vs-based liquefaction evaluation procedure is evaluated using Vs profiles obtained directly via surface wave methods (i.e., Vs-SW) and generated indirectly using the Christchurch-specific Vs correlation based on CPT tip resistance (i.e., Vs-CPT) developed by McGann et al. (2015a). The predictive capabilities of each of the two Vs-based liquefaction evaluation procedures are quantitatively evaluated based on the error index proposed by Green et al. (2014).

Herein, information on the geology and geomorphology of the Canterbury Plains is discussed first, with particular emphasis on information relevant to liquefaction potential. Next, the ground motions recorded during the Canterbury earthquake sequence are briefly discussed and provide information regarding how the peak ground accelerations (PGAs) at each site were estimated from strong motion records of the Darfield and Christchurch earthquakes. This is followed by an explanation of how the Vs profiles were developed at each site using surface wave methods and how the correlated Vs profiles were developed from CPT logs. Finally, the Andrus and Stokoe (2000) and Kayen et al. (2013) procedures are evaluated in aggregate, followed by a detailed discussion of the results at 2 of the 23 sites that reinforces the findings of the study. An extensive electronic supplement is provided that will allow future researchers to make their own interpretations of the case histories if they desire to do so.

Geology and Recorded Ground Motions

Christchurch is located along the eastern portion of overlapping alluvial fans formed by glacial-fed rivers emanating from the Southern Alps, which run north-south across the southern island of New Zealand. The alluvial fans form the Canterbury Plains, which are approximately 160 km long and up to 60 km wide (Forsyth et al. 2008). Alluvial deposits in the Canterbury Plains vary in thickness from at least 500 m to over 1,000 m (Brown et al. 1995). These deposits consist of alternating layers of gravels and silty sands that are derived from the greywacke of the Southern Alps and from windblown loess.

The greater Christchurch area lies within the modern-day floodplain of the Waimakariri River and is underlain by abandoned and infilled channels of the Waimakariri and two local spring-fed rivers, the Avon and the Heathcote. The locations of these abandoned and modern-day river channels are of particular importance for liquefaction and lateral spreading and are often associated with young (Holocene-age) loose and soft sediments, characterized by shallow groundwater levels (1–5 m below the ground surface) and highly susceptible to liquefaction (e.g., Wotherspoon et al. 2012). Samples of liquefaction ejecta recovered following the earthquake are described as silty fine sand having subrounded angular shapes made predominately from quartz and feldspar (Green et al. 2014).

The 2010–2011 CES began with the September 4, 2010, M_w 7.1 Darfield earthquake (Bradley et al. 2014). It was followed by three 3 with $M_w \ge 5.9$ and up to 10 events in the sequence were large enough to trigger liquefaction in the region (Quigley et al. 2013). The Darfield earthquake resulted in significant damage to the built environment and induced widespread liquefaction in eastern Christchurch and Kaiapoi (a small city north of Christchurch) (Cubrinovski et al. 2010). Despite the widespread damage from the Darfield earthquake, no fatalities or major injuries were recorded. The most damaging of the earthquakes was the February 22, 2011, M_w 6.2 Christchurch earthquake, which caused significant shaking damage to commercial and residential buildings, induced widespread liquefaction throughout Christchurch, and resulted in 185 fatalities (Cubrinovski et al. 2011; Green et al. 2011; Buchanan et al. 2011). The ground motions from the event exceeded the design response spectra in Christchurch for structures with a range of fundamental periods, primarily because of the close proximity of the fault rupture to the city (Bradley et al. 2014).

The Darfield and Christchurch ground motions were recorded by a dense network of strong motion stations throughout the Christchurch regions (Cousins and McVerry 2010; Bradley and Cubrinovski 2011; Bradley 2012b; Bradley et al. 2014). The ground motions were used to estimate the PGA at each site, which was combined with earthquake magnitude to estimate the amplitude and duration of cyclic loading per the simplified liquefaction procedures investigated in this study. The method used to estimate the conditional PGA distribution in the Canterbury region and develop the PGA for each case history site is outlined in Green et al. (2014) and detailed further in Bradley (2014).

Development of Liquefaction Case Histories

Case history sites for this study were chosen from those compiled by Green et al. (2014), which consisted of 25 sites analyzed for both the Darfield and Christchurch earthquakes (25 sites \times 2 events = 50 case histories). These 25 sites were originally selected by Green et al. (2014) because they experienced severe or moderate surficial liquefaction manifestation in one event and no or minor surficial liquefaction manifestation in the other event. Thus, these sites would seemingly yield case histories that would best constrain the position of the CRR curve. Sites were also chosen for their close proximity (within -1.65 km) to strong motion stations to reduce the uncertainty in the PGA estimates.

Out of the 25 sites investigated by Green et al. (2014), 23 were chosen for analysis in the present study. The site numbers in this study remain the same as those presented in Green et al. (2014). The 23 sites are tabulated in Table 1, and their positions are superimposed on an aerial image showing liquefaction manifestations that resulted from the Darfield and Christchurch earthquakes in Fig. 1. Two sites compiled by Green et al. (2014) were not used herein because their CPT soundings were significantly different from their Vs profiles. The differences are attributed to lateral variability (e.g., Vs profiles had to be measured away from the location of the CPT because of site constraints) and would have resulted in poor case histories.

Each of the 23 sites was visited and revisited by the authors following the Darfield and Christchurch earthquakes and during

Table 1. Case History Site Locations and Site Information

Site number	Site name ^a	Latitude (degrees)	Longitude (degrees)	Critical depth range (m)	GWT ^b depth (m)	σ_{V0}^{c} (kPa)	σ'_{V0}^{c} (kPa)	Apparent F_C^{d} (%) R&W98
1	SHY-09	-43.50517	172.65922	3.80-5.75	2.0	88.1	60.9	4.8
2	AVD-07 alt	-43.50852	172.68702	1.80-3.00	1.7	42.6	35.7	16.1
3	BUR 46	-43.49815	172.70025	5.75-8.75	1.3	138.1	79.8	8.9
4	CBD 21 alt	-43.52435	172.63265	1.40-1.82	1.4	27.9	25.8	18.8
5	FND 01	-43.52393	172.61217	3.60-3.90	1.8	66.5	47.9	15.4
6	KAN 03 alt	-43.38132	172.66673	1.60-3.50	1	47.2	32	17.7
7	KAN 05	-43.38300	172.65913	3.15-4.10	2.0	65.7	49.7	7.3
8	KAN 09	-43.38137	172.66148	1.25-2.45	0.9	33.8	24.5	7.4
9	KAN 19	-43.38057	172.66871	2.35-5.00	0.8	69.7	41.5	5.9
10	KAN 23	-43.38098	172.67360	4.30-5.30	0.5	92.4	50.2	6.0
11	KAN 26d ^e	-43.38087	172.65688	4.90-8.00	1.5	122.0	73.5	6.2
11	KAN 26c ^e	-43.38087	172.65688	1.50-2.40	1.5	34.3	29.9	14.3
12	KAN 28	-43.38153	172.65773	2.00-3.15	1.4	46.7	35.2	5.3
14	KAS 11	-43.38818	172.66213	2.00-3.10	1.2	46.7	33.5	10.6
15	KAS 20 alt	-43.37935	172.64838	2.00-3.50	1.6	49.6	38.3	11.5
17	SNB 01	-43.49640	172.70278	2.25-5.00	2.0	65.7	49.7	9.7
18	NBT 02	-43.49737	172.70437	4.80-6.70	2.0	107.1	70.3	10.4
19	NBT 03 alt	-43.49897	172.70525	$5.00-7.00^{\mathrm{f}}$	2.4	144.2	92.2	10.1
20	RCH 14 alt	-43.50310	172.66185	2.70-5.50	2.3	74.0	56.3	6.4
21	Z1-3	-43.52655	172.63847	4.00-8.25	1.4	115.9	69.6	17.5
22	Z2-4	-43.52833	172.63532	$1.10-2.10^{\rm f}$	1.0	51.1	34.0	10.5
23	Z2-6	-43.52763	172.63697	2.00-2.85	2.0	42.3	38.1	13.6
24	Z4-4	-43.52875	172.64227	2.00-3.25	2.0	46.2	40.1	14.1
25	Z4-4 (2)	-43.52852	172.64328	2.00-3.25	2.0	46.2	40.1	14.1

^aDesignation "alt" indicates alternative site interpretation.

data collection for the study. Classifications regarding severity of liquefaction/liquefaction manifestations at each site were based on personal observations, aerial photographs following each event, and/or interviews with residents during the data collection. Detailed explanations of the liquefaction manifestations at each site are provided in the Supplemental Data and in the electronic supplement provided with Green et al. (2014).

For the majority of the 23 Vs case histories discussed here, the critical layer identified by Green et al. (2014) based on CPT data was used. These critical layers were developed with the guiding principle that the depth-thickness-density combination of the critical layer for a given site should be consistent with the observed liquefaction response of the site (Green et al. 2014, 2005; Olson et al. 2005; Green and Olson 2015). Initially many sites were considered for both the Green et al. (2014) study and this study. However, some sites were removed from consideration because of significant uncertainties in the locations and representative properties needed to define the critical layers (e.g., critical layers between interbedded gravels where accurate CPT tip resistance and Vs estimates were less reliable). For sites where no surficial evidence of liquefaction was observed, the critical layer was taken as the layer believed to be the most susceptible to liquefaction based on the CPT data. Because of ambiguity in the selection of a single critical layer at a few sites, Green et al. (2014) selected an alternative critical layer in addition to the preferred critical layer. For this study, only the critical layer that provided the most advantageous results for the two Vs-based liquefaction evaluation methods was considered. The sites where the alternative CPT-based critical layer was used are listed in Table 1 with an "alt" designation. For two cases (NBT 03 alt and Z2-4), the location of the critical layers was adjusted slightly to provide a better match with abrupt changes in the surface wave-derived Vs profiles. For the NBT 03 alt site, the thickness of the critical layer was reduced by half because of an increase in the Vs-SW profile that was not mirrored in the nearby CPT tip resistance (q_c). For the Z2-4 site, an alternative CPT was used for the interpretation, which was closer to the location of the surface wave testing and agreed better with the Vs-SW profile than the CPT used in Green et al. (2014). Additional information on the selection of the critical layers at each site can be found in Green et al. (2014).

Development of Shear-Wave Velocity Profiles

Shear-wave velocity profiles were developed at each of the 23 case history sites using two methods: (1) surface wave measurements made by the authors at each site (referred to as Vs-SW) and (2) a Christchurch-specific Vs correlation based on CPT tip resistance developed by McCann et al. (2015a) (referred to as Vs-CPT) using the CPT soundings documented in Green et al. (2014). The surface wave testing was conducted as close as practical (typically within 0–50 m) to the CPT location to ensure that similar materials were measured by each method. The relative location of the surface wave array compared with the CPT location for each site is provided in the Supplemental Data for this paper.

Shear-Wave Velocity Profiles from Surface Wave Testing

Surface wave testing at each site involved a combination of active-source techniques—spectral analysis of surface waves (SASW) and multichannel analysis of surface waves (MASW)—and

^bDepth of GWT estimated from P-wave refraction and CPTu data.

^cVertical stresses computed assuming soils above and below GWT had total unit weights of 17.0 and 19.5 kN/m³, respectively.

^dFines content estimated from CPT soundings using Robertson and Wride (1998).

eKAN-26d and KAN-26c list data for KAN-26 for Darfield (d) and Christchurch (c) earthquakes, respectively.

^fSite where critical layers adjusted from those provided in Green et al. (2014).

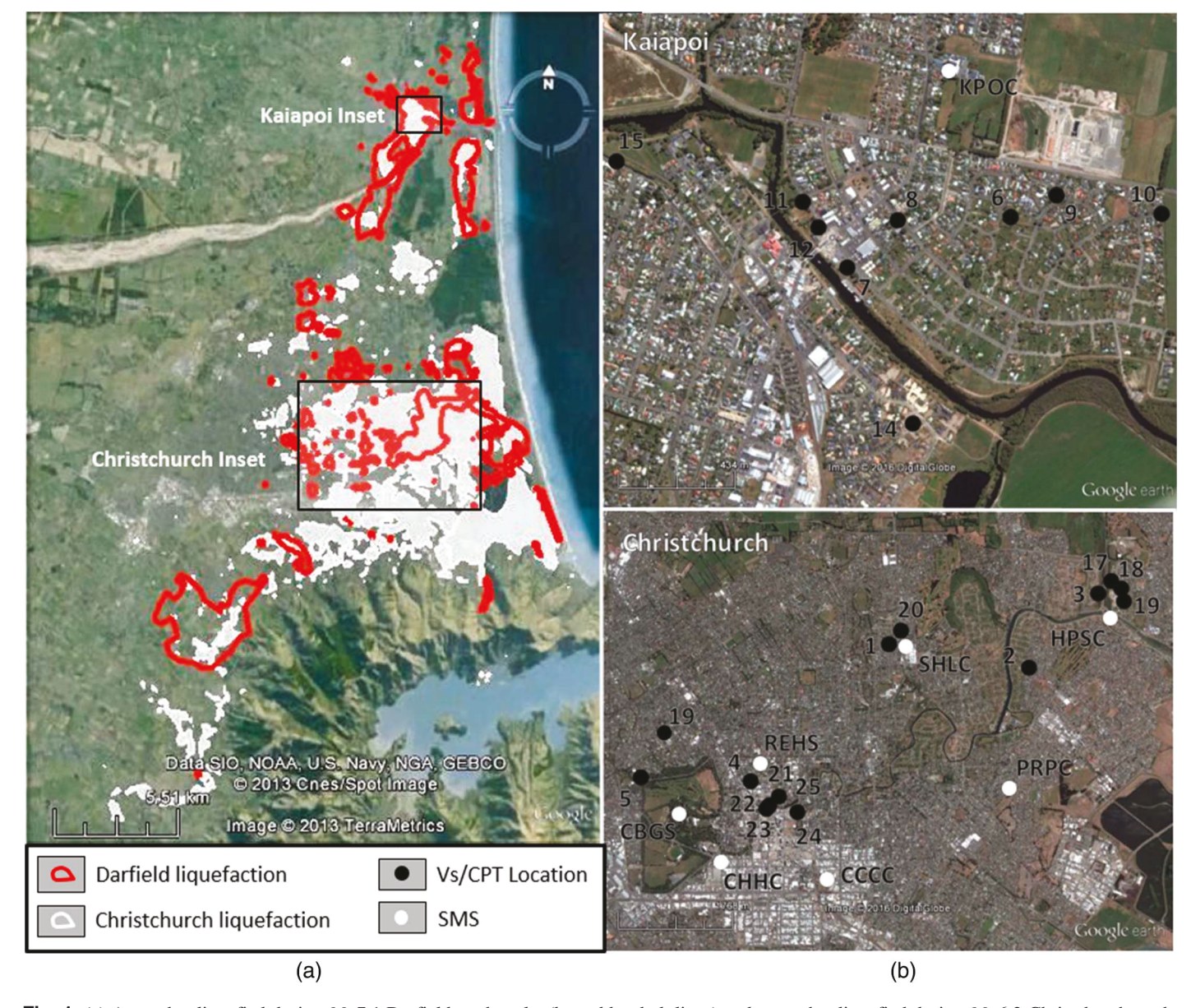


Fig. 1. (a) Areas that liquefied during M_w 7.1 Darfield earthquake (bound by dark lines) and areas that liquefied during M_w 6.2 Christchruch earthquake (white shaded areas); (b) locations of case history sites (numbered, black circles) and strong motion seismograph stations (labeled, white circles) [(a and b) modified from Green et al. 2014, with permission from the Earthquake Engineering Research Institute; (a) base map image © 2013 TerraMetrics; data SIO, NOAA, U.S. Navy, NGA, GEBCO © 2013 Cnes/Spot Image; (b) base map image © 2016 DigitalGlobe]

passive-source techniques—one-dimensional (1D) and two-dimensional (2D) microtremor array measurements (MAMs). Active-source linear array (1D) testing employed a receiver array composed of 24, 4.5-Hz geophones with an equal spacing (d_x) of either 0.9 or 1.5 m (a total array length of either 20.7 m or 34.5 m, respectively). The same linear array was used to collect passive-source data (refraction microtremor, ReMi) for comparison purposes. Where possible, an L-shaped array with receivers placed at 1.5-m intervals was also used for passive-source 2D MAM measurements. For active-source testing, a 5.4-kg sledgehammer was used to generate surface wave energy.

At sites with surface soil conditions, a P-wave refraction survey was performed using the linear array (P-wave refraction could not be conducted at sites with asphalt at the surface). These measurements were used to determine the depth to 100% saturation (assumed to coincide with the groundwater table) at each site for input into the surface wave inversion and liquefaction analyses.

The pore pressure logs from the CPT soundings were used to determine the water table depth in cases where P-wave refraction could not be used. For refraction testing, five hammer blows (shots), located one receiver spacing in front of the first receiver, were stacked to increase the signal-to-noise ratio. At this same source location, SASW data were collected using select pairs of geophones in the linear array of 24 geophones. Typical SASW receiver spacings included $1d_x$, $2d_x$, $3d_x$, $4d_x$, $6d_x$, $8d_x$, $10d_x$, and $12d_x$, where d_x is the spacing between geophones (resulting in minimum SASW receiver spacings of approximately 0.91 or 1.52 m and maximum receiver spacings of approximately 11 or 18.3 m). These pairs of receivers were always chosen to maintain the distance between the source and first receiver equal to the distance between the first and second receiver, as is typical to avoid near-field effects in SASW testing (Stokoe et al. 1994). Following the SASW data collection, MASW testing was performed using three separate source locations of 4.6, 9.1, and 18.3 m from the

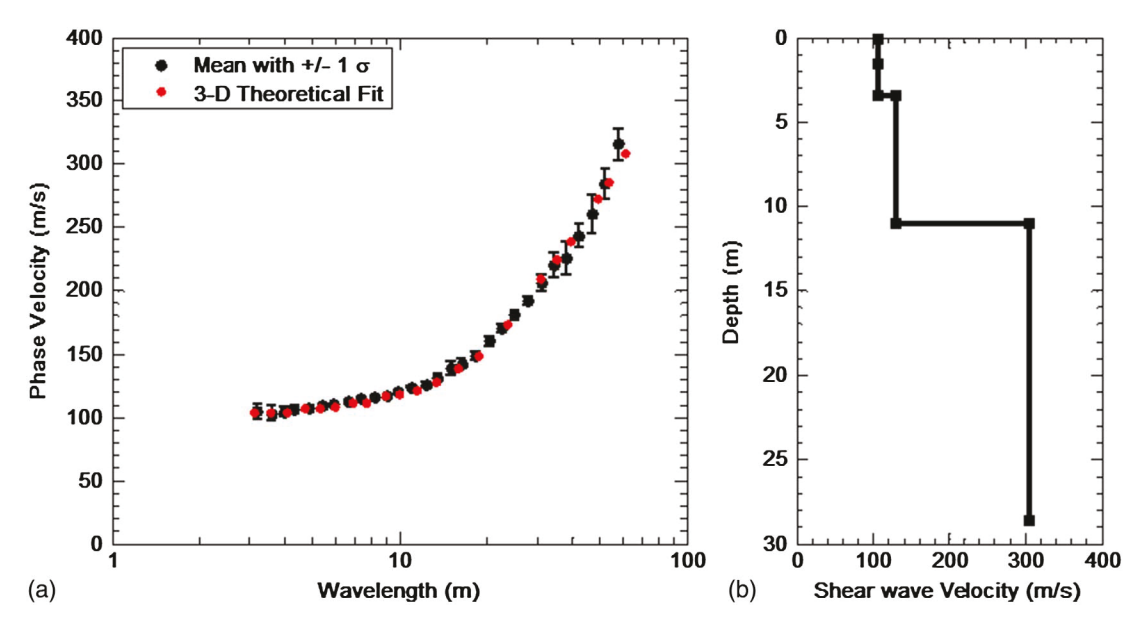


Fig. 2. Surface wave results for Site 11: KAN 26: (a) experimental dispersion curve with associated uncertainty along with matching theoretical dispersion curve; (b) shear-wave velocity profile corresponding to theoretical dispersion curve

first receiver in the array, as a means to mitigate against near-field effects, resulting in array-center distances of 22.1, 26.6, and 35.8 m (Yoon and Rix 2009). As with the P-wave refraction, at least five sledgehammer blows were stacked at each source location during surface wave testing to increase the signal-to-noise ratio.

Linear array passive surface wave testing [i.e., ReMi, as described in Louie (2001)] was conducted using the same array used for active testing. During passive testing, a total of 10, 32-s-long noise signals were recorded. Then, at some sites where space allowed, the linear array was converted into a 2D array by rotating 12 of the 24 geophones by 90° , resulting in a 16.7×18.2 -m L-shaped array. The 2D passive array has several advantages over a linear passive array, the most important of which is the ability to resolve the direction of surface wave propagation. The lack of directional information when using a linear passive array can lead to significant errors in velocity profiles under certain circumstances, and caution should be exercised when using this method without other corroborating active or 2D passive methods (Cox and Beekman 2011).

The surface wave data were analyzed to develop individual dispersion curves for each of the surface wave methods described previously. The SASW data were analyzed using the phase unwrapping method to determine individual dispersion curves from each receiver spacing. The individual dispersion curves were then combined to form a composite dispersion curve over the frequencies/ wavelengths of interest. The MASW data were analyzed using the frequency domain beamformer method (Zywicki 1999). For each source offset, a dispersion curve was generated by picking the maximum spectral peak in the frequency-wavenumber domain. The linear array passive data were analyzed using the 2D slownessfrequency (p-f) transform in the software SeisOpt ReMi. The 2D MAM data were analyzed using the 2D frequency domain beamformer method (Zywicki 1999). Additional information about the general surface wave-processing methods can be found in Cox and Wood (2011).

Once the surface wave dispersion trends from each method (i.e., SASW, MASW, and MAM) were obtained, a mixed-method composite dispersion curve was generated by combining the dispersion data from each active and passive surface wave method.

The dispersion data were then divided into 30 wavelength bins equally spaced in terms of a log distribution. The mean phase velocity and associated standard deviation were then calculated for each bin, resulting in an experimental dispersion curve with associated uncertainty [Fig. 2(a)]. The shear-wave velocity profile was then determined by fitting a "3D" theoretical solution to the mean experimental dispersion curve using the software WinSASW (Joh 1996) [Figs. 2(a and b)]. The "3D" solution uses the superposed-mode dynamic stiffness matrix method to solve for the surface displacements generated by all Rayleigh wave modes and body waves (Joh 1996). This effective mode solution is the most appropriate one for SASW and can also be used to account for the smearing/superposition of modes that can exist in MASW dispersion data at longer wavelengths because of a lack of spatial resolution. The shear-wave velocity profiles obtained from the inversions for each site were limited to the maximum experimental wavelength divided by two (i.e., $\lambda_{\text{max}}/2$).

To ensure a robust solution to the inverse problem (i.e., theoretical fit to the experimental dispersion curve), a top-down forward modeling approach informed by the layering indicated in nearby CPT results was employed. In this approach, the initial inversion models consisted of a single, half-space layer and only the shortwavelength portion of the experimental dispersion curve was fit. Additional layers were then added when (1) they were shown to exist in the CPT measurements and/or (2) they were required to match the shape of the experimental dispersion curve. This topdown approach, informed by the layering indicated in nearby CPT results, helped to prevent errors in deeper layers from corrupting the velocity of shallow layers. However, the inversion model layering was allowed to differ from the CPT layering when required to fit the experimental dispersion data. This can be necessary because of (1) differences in the spatial locations of the surface wave and CPT tests, (2) spatial averaging of properties within the extent of the surface wave array versus essentially point measurements with the CPT, and (3) fundamental differences in the small-strain stiffness sensed by surface wave measurements and the large-strain density/strength sensed by CPT tip resistance.

During this initial portion of the forward modeling process, the match between the experimental dispersion data and the theoretical dispersion curve was evaluated by eye rather than by use of a single dispersion misfit value. While dispersion misfit values are commonly used to quantify the goodness of fit during blind global inversions, it is important to recognize that dispersion misfit values deemed to be satisfactory at one site may be considered mediocre or poor at another site because of complexity of the experimental dispersion curve in the form of mode jumps and dispersion uncertainty (Cox and Teague 2016). Thus, an experienced analyst must always ensure that theoretical dispersion curves visually match the experimental dispersion data in the areas of greatest interest while simultaneously trying to minimize a dispersion misfit value, which represents a single, average error across the entire bandwidth of the dispersion curve. After a good Vs profile was developed through visual inspection and top-down iterative forward modeling, a leastsquares automated inversion, available in WinSASW, was used to refine the results to obtain the final "best" Vs profile for each site. The Vs profiles developed in this manner are expected to be as accurate as possible, given the uncertainties involved in surface wave inversion and spatial averaging that occur in the extents of the array.

Although CPT soundings were used to inform the choice of layering (thickness and depth) during the surface wave inversion process, one should not expect perfect agreement between the CPT layering and the Vs layering. For example, the soil characteristics that strongly influence the measured CPT tip resistance (q_c) differ from those that strongly influence Vs (e.g., q_c is very sensitive to density, whereas Vs is far less sensitive and Vs is very sensitive to microstructure, whereas q_c is far less sensitive). In addition, q_c may drastically increase in sands with gravel because of gravel-to-tip impacts, yet the change in small-strain Vs will be much more subdued because the global stiffness of the material is governed by the soil matrix. Thus, one expects general agreement, not perfect agreement, between the two methods. Apparent differences in the layering between CPT and Vs-SW do not necessarily mean one method is right and one method is wrong. Rather, they are different, and some visible differences between the CPT and Vs-SW profiles are evident both in the current data set and in other data sets documented by the authors (e.g., Wotherspoon et al. 2013).

The Christchurch Vs data set also presents a unique challenge in terms of modeling the near-surface layering at each site based on surface wave results. Surface conditions for testing varied, with 13 sites on grass/soil, 2 on thin asphalt sidewalks, and 8 on asphalt pavements. Regardless of the surface layering conditions, one should not attempt to resolve near-surface layers during surface wave inversion that are thinner than the minimum wavelength divided by approximately two or three (Garofalo et al. 2016b; Cox and Teague 2016). To do so, implies resolution that does not exist in the method. Given that minimum experimental wavelengths were typically on the order of 1 m, surface layers less than 30-50 cm thick could not be accurately resolved. Hence, pavement and base layers were often grouped together as a single layer with an "average" Vs during inversion. Although the absolute layering in the near surface cannot be recovered using such an approach, the velocities and layering deeper in the profile (i.e., at depths greater than approximately 1.5-2 times the minimum wavelength) should not be seriously compromised as long as the experimental dispersion data at the shortest wavelengths are matched during inversion. However, because a lack of short-wavelength data can lead to uncertainties in the SW-Vs, especially for pavement sites, it is always advisable to collect dispersion data with wavelengths as short as reasonably possible to ensure that accurate velocities are developed for the critical layers. The lack of very shortwavelength data (<1 m wavelength) at pavement sites is a source of potential uncertainty in some of the SW-Vs profiles developed in this study, although the authors believe that the critical layers are deep enough to minimize this uncertainty. Furthermore, asphalt pavements at most of the sites in Christchurch, especially those in subdivisions and on small collector streets, are composed of a thin chip seal layer over a moderate base course. These thin pavement layers, when combined with the significant liquefaction damage that occurred during the earthquakes, resulted in surface layers that were much softer than traditional, undamaged pavements. A full description of the experimental data, theoretical fits, and inverted profiles can be found for each site in the Supplemental Data.

Shear-Wave Velocity Profiles Correlated from CPT

A Christchurch-specific correlation relating CPT tip resistance and Vs was developed by McGann et al. (2015a) and used in conjunction with the data set of CPT soundings presented in Green et al. (2014) to develop a second set of Vs estimates at each of the 23 sites. The McGann et al. (2015a) correlation was developed using 86 seismic CPT (SCPT) logs where the Vs was derived from the travel time analysis of vertically propagating shear waves. The resulting correlation was used to develop a model to estimate Vs from the tip resistance (q_c) and the sleeve friction (f_s) without the need to conduct SCPT. The CPT-Vs correlation is given as Eq. (1):

$$Vs = 18.4q_c^{0.144} f_s^{0.0832} z^{0.278}$$
 (1)

where Vs = shear-wave velocity (m/s); q_c = raw cone tip resistance (kPa); f_s = raw frictional resistance (kPa); and z = depth below ground surface (m).

An estimate of the standard deviation for the model is provided; however, this estimate was not directly used in this study. In addition to the calibration data set of SCPT, McGann et al. (2015b) compared Vs profiles generated using Eq. (1) with surface wave-generated Vs profiles collected at SMSs in Christchurch (Wood et al. 2011, 2015; Wotherspoon et al. 2015). In most cases, the Vs profiles showed good agreement at intermediate depths (6-20 m). However, the CPT-Vs correlation was shown to yield lower estimates of Vs in the near surface (z < 6 m) and higher estimates of Vs at deeper depths (z > 20 m) in comparison with the Vs-SW. The higher values of Vs-CPT at depths greater than 20 m were determined by McGann et al. (2015b) to be caused by the cone encountering the Riccarton Gravel formation at the bottom of each CPT profile, which led to erroneously high results for CPT tip resistance. The cause of the bias between the methods in the near surface (z < 6 m) was not determined with strong certainty.

It is expected that the Vs-CPT profiles will more closely match the critical layering determined by Green et al. (2014) because they are directly based on a correlation with the CPT data whereas the Vs-SW profiles are based on independent measurements that investigate average soil properties over a much larger extent (20–30 m). Moreover, surface wave measurements typically suffer from decreasing layer resolution with depth whereas CPT resolution remains relatively constant with depth. These factors result in the Vs-CPT profiles providing a localized-fine Vs profile whereas the Vs-SW profiles provide a more global-coarse Vs profile.

Evaluation of Vs-Based Liquefaction Triggering Procedures

The 46 Vs liquefaction case history data points developed in this study were used to evaluate the Andrus and Stokoe (2000) (A&S00) and Kayen et al. (2013) (KEA13) Vs-based simplified liquefaction evaluation procedures in a deterministic fashion. Although the KEA13 procedure is presented in a probabilistic

framework, the present paper focuses only on the deterministic approach, which is associated with a probability of liquefaction of 15%. For the A&S00 procedure, the fines content (FC) of each critical layer was determined based on the I_c -FC correlation (i.e., soil behavior-type index to fines content) proposed by Robertson and Wride (1998). The Christchurch soil–specific Ic-FC correlation developed by Robinson et al. (2012) was also evaluated, but, as determined in Green et al. (2014), the generic correlation by Robertson and Wride (1998) provided better results for the cases analyzed. The better performance of the generic I_c -FC correlation may not hold true in other areas, but for this paper the Robertson and Wride (1998) results only are presented. For more information on these calculations see Green et al. (2014).

Representative values for the cyclic stress ratio (CSR), CRR, Vs1, factor of safety, and error index for the critical layer for each case history are tabulated in the accompanying Supplemental Data. These representative values were obtained by first computing each parameter for the entire profile depth and then averaging each parameter across the critical layer. This procedure is technically more appropriate than averaging the Vs values across the critical layer and then using the average value of Vs to compute representative CSR, CRR, and Vs1 values for the critical layer. The use of an average value of Vs in the critical layer to compute the CSR, CRR, and Vs1 does not take into account the nonlinear nature of the overburden stress correction and stress reduction

factor (r_d) . Therefore, if the CRR values are computed using the average Vs1 values provided in the Supplemental Data, they may differ slightly from the representative CRR values provided in the tables.

In Fig. 3, the case history data are plotted along with the CRR curves for a $M_W7.5$ earthquake (i.e., $\text{CRR}_{M7.5}$) and for a 1-atm initial vertical effective confining stress (σ'_{vo}) for the two Vs-based liquefaction evaluation procedures (A&S00 and KEA13) and the two methods for obtaining Vs profiles (i.e., Vs-SW and Vs-CPT). The Vs-SW data analyzed using the A&S00 and KEA13 procedures are plotted in Figs. 3(a and b), respectively. The Vs-CPT data analyzed using the A&S00 and KEA13 procedures are plotted in Figs. 3(c and d), respectively. To evaluate the predictive performance of the triggering relationships for each dataset, the error index (E_I) originally proposed by Green et al. (2014) was used:

$$E_I = \sum_{i=1}^n W f_i * E_i \tag{2}$$

where n = number of case histories; Wf_i = weighting factor based on observed occurrence (or nonoccurrence) of liquefaction at the site; and E_i = relative error value for a given site/Vs profile/triggering method.

The E_I is the combined error of all similar case histories, which is calculated as

$$E_i = \begin{cases} 1.0 \cdot |\mathsf{CSR}_{M7.5} - \mathsf{CRR}_{M7.5}| & \text{for "Liq" cases where } \mathsf{CSR}_{M7.5} < \mathsf{CRR}_{M7.5} \\ 0 & \text{for "Liq" cases where } \mathsf{CSR}_{M7.5} \ge \mathsf{CRR}_{M7.5} \end{cases}$$

$$E_i = \begin{cases} 0.75 \cdot |\mathsf{CSR}_{M7.5} - \mathsf{CRR}_{M7.5}| & \text{for "Minor Liq" cases where } \mathsf{CSR}_{M7.5} < \mathsf{CRR}_{M7.5} \\ 0 & \text{for "Minor Liq" cases where } \mathsf{CSR}_{M7.5} \ge \mathsf{CRR}_{M7.5} \end{cases}$$

$$E_i = \begin{cases} 0.5 \cdot |\mathsf{CSR}_{M7.5} - \mathsf{CRR}_{M7.5}| & \text{for "No Liq" cases where } \mathsf{CSR}_{M7.5} > \mathsf{CRR}_{M7.5} \\ 0 & \text{for "No Liq" cases where } \mathsf{CSR}_{M7.5} \le \mathsf{CRR}_{M7.5} \end{cases}$$

"Liq," "Minor Liq," and "No Liq" in the expressions for E_i correspond to cases where the observed surficial liquefaction manifestations were moderate to severe, minor, and not observed, respectively, as defined by Green et al. (2014). The proposed E_i behaves such that if all case histories are correctly predicted (i.e., field observations match triggering predictions), it equals zero. However, as the number and "magnitude" of the mispredictions increase, E_i also increases. For individual cases, E_i equals zero for a correct prediction of "Liq," "Minor Liq," and "No Liq," but is proportional to the vertical distance between the plotted point and the $CRR_{M7.5}$ curve (i.e., the error) for mispredicted cases. To acknowledge the varying significance of the consequences of mispredicting cases in each of the severity categories (i.e., "Liq," "Minor Liq," and "No Liq"), weighting factors (Wf_i) are included in E_i : 1.0 for mispredicted "Liq" cases, 0.75 for mispredicted "Minor Liq" cases, and 0.5 for mispredicted "No Liq" cases. Green et al. (2014) used two sets of weighting factors in analyzing the CPT case histories. The first set, presented in the main text of Green et al. (2014), assumes values of 1.0 for all mispredictions independent of the severity of the surficial liquefaction manifestations. The second set, presented in the electronic supplement of Green et al. (2014), are the same as those used here.

The E_is and relative performance of each method are first examined using two example case histories (Site 23: Z2-6 and Site 24: Z4-4). These examples illustrate scenarios where the KEA13 procedure outperforms the A&S00 procedure, resulting in lower E_is . They also highlight some potential shortcomings of the CPT-Vs correlation in regard to false-positive liquefaction predictions. Following these detailed discussions at two example sites, trends from the entire data set are examined and discussed.

Example Case History 1 (Site 23: Z2-6)

Site 23: Z2-6 is located at the southeast corner of the intersection of Oxford Terrace and Colombo Street in the Christchurch central business district (CBD). The site is just to the south of the Avon River. It is approximately 0.65 km from the Christchurch resthaven (REHS) strong motion seismograph station, and the estimated

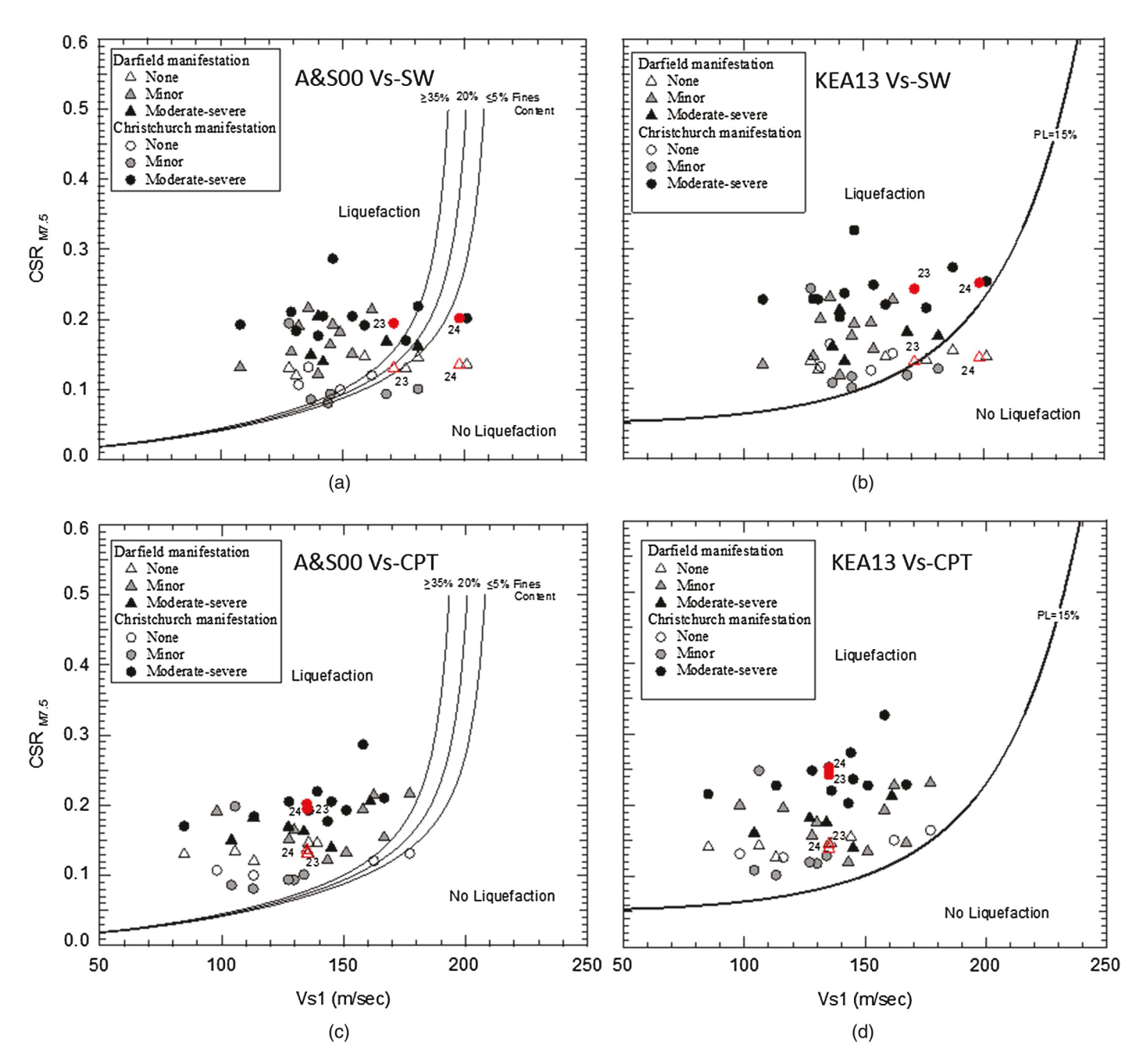


Fig. 3. Case history data plotted with CRR_{M7.5} curves: (a) A&S00 Vs-SW; (b) KEA13 Vs-SW; (c) A&S00 Vs-CPT; (d) KEA13 Vs-CPT; Sites 23 and 24 are labeled

geometric means of the horizontal PGAs at the site during the Darfield and Christchurch earthquakes are 0.21 and 0.45g, respectively. There were no observed surface manifestations of liquefaction at the site following the Darfield earthquake. However, there was significant lateral spreading at the site following the Christchurch earthquake. Site photographs, figures, and tabulated data can be found in the Supplemental Data.

In Fig. 4, the CPT cone tip resistance normalized to one atmosphere and corrected for fines content to a clean sand equivalent (q_{c1Ncs}) , I_c , Vs and Vs1, and CSR and CRR for both the A&S00 and KEA13 procedures are plotted as a function of depth for both the Vs-SW and Vs-CPT profiles for Site 23: Z2-6. The critical layer, determined by Green et al. (2014), is located 2.00–2.85 m below the surface with the water table at 2.0 m. For the Vs-SW profile, the average Vs1 for the critical layer is 171 m/s. Both

the A&S00 and KEA13 procedures correctly yield predictions that match the lack of observed surface manifestations of liquefaction at the site for the Darfield earthquake, with factors of safety of 1.16 and 1.19, respectively, when using the Vs-SW profile (refer to summary tables in the Supplemental Data and the relative positions of the data points for Site 23 in Fig. 3). For the Christchurch earthquake, both the A&S00 and KEA13 procedures correctly yield predictions that match the observations of liquefaction at the site, with factors of safety of 0.78 and 0.68, respectively, when using the Vs-SW profile. Thus, the E_i values for the Vs-SW profile are zero for both analysis methods because all predictions correctly match observations. However, for the Vs-CPT profile, the average Vs1 for the critical layer is 135 m/s (36 m/s less than the Vs-SW value). Thus, both the A&S00 and KEA13 procedures incorrectly yield predictions of liquefaction at the site for the Darfield earthquake

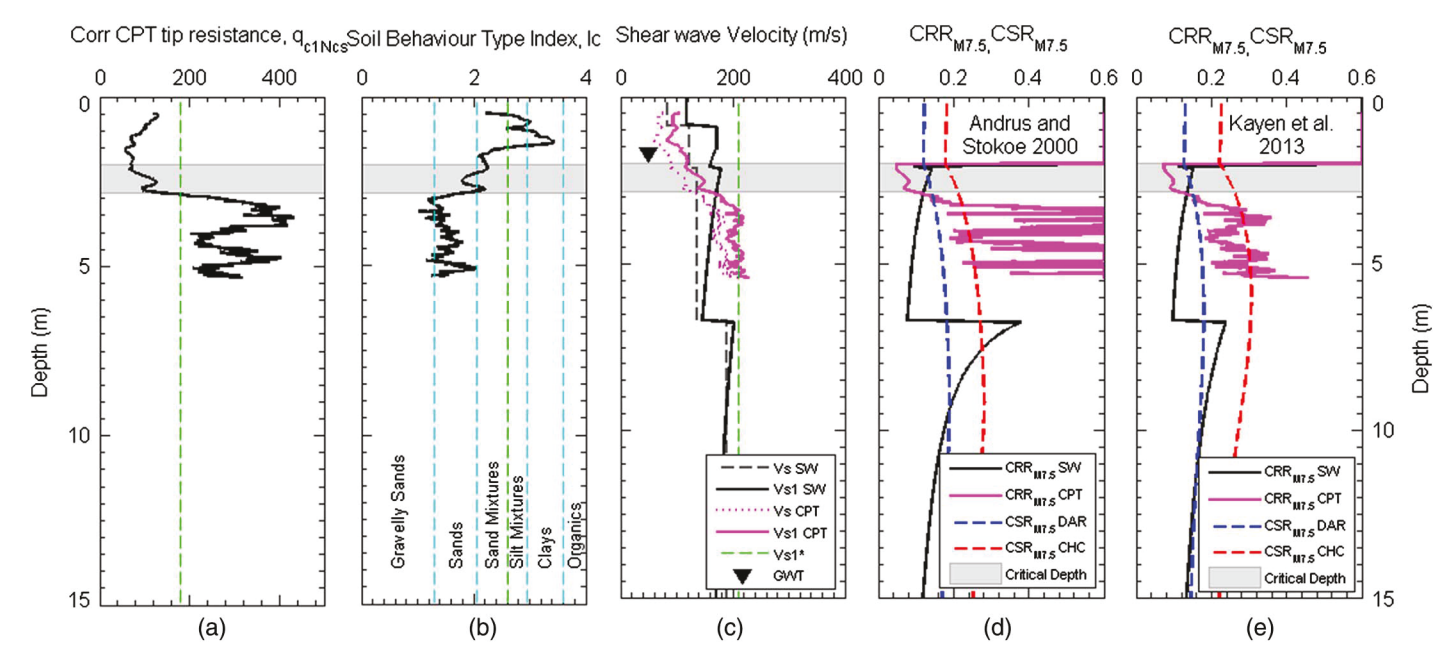


Fig. 4. (a) Corrected CPT tip resistance (q_{c1Ncs}) ; (b) soil behavior-type index (I_c) ; (c) raw and corrected Vs for SW and CPT (Vs and Vs1); (d) cyclic resistance ratio (CRR_{M7.5}) for SW and CPT; (e) cyclic stress ratio (CSR_{M7.5}) and Darfield and Christchurch earthquakes for Site 23: Z2-6; Vs1 shown is from A&S00 relationship

(based on observed surface manifestations), with factors of safety of 0.55 and 0.67, respectively, when using the Vs-CPT profile. These false-positive mispredictions result in E_i values of 0.03 and 0.023, respectively, for the A&S00 and KEA13 procedures. However, for the much higher PGA associated with the Christchurch earthquake, both the A&S00 and KEA13 procedures correctly predict the occurrence of liquefaction at the site, with factors of safety of 0.37 and 0.39, respectively, when using the Vs-CPT profile. Hence, the E_i error values are equal to zero for both triggering methods when considering the Christchurch earthquake. For comparison, Green et al. (2014) showed that the Idriss and Boulanger (2008) CPT liquefaction triggering procedure correctly predicted the observed performance at the site during both the Darfield and Christchurch earthquakes.

Example Case History 2 (Site 24: Z4-4)

Site 24: Z4-4 is located at the northwest corner of the intersection of Armagh Street and Madras Street in Christchurch's CBD. The site is approximately 200 m south of the Avon River. It is approximately 0.95 km from the REHS strong motion seismograph station, and the estimated geometric means of the horizontal PGAs at the site during the Darfield and Christchurch earthquakes are 0.21 and 0.45g, respectively. There were no observed surface manifestations of liquefaction at the site following the Darfield earthquake. However, there was evidence of moderate liquefaction at the site following the Christchurch earthquake. Sitephotographs, figures, and tabulated data can be found in the Supplemental Data.

In Fig. 5, the q_{c1Ncs} , I_c , and Vs and Vs1, and CSR and CRR for both the A&S00 and KEA13 procedures are plotted as a function of depth for both the Vs-SW and Vs-CPT profiles for Site 24: Z4-4. The critical layer, determined by Green et al. (2014), is located 2.00–3.25 m below the surface with the water table at 2.0 m. For the Vs-SW profile, the average Vs1 for the critical layer is 198 m/s. Both the A&S00 and KEA13 procedures correctly yield predictions that match the lack of observed surface manifestations

of liquefaction at the site for the Darfield earthquake, with factors of safety of 2.39 and 1.61, respectively, when using the Vs-SW profile (refer to summary tables in the electronic supplement and the relative positions of the data points for Site 24 in Fig. 3). Thus, the E_i values associated with the Vs-SW profile are zero for both methods of analysis when considering the Darfield earthquake. However, for the Christchurch earthquake, the A&S00 procedure yields a factor of safety of 1.62, resulting in an incorrect prediction of no liquefaction at the site and a false-negative E_i of 0.125. On the other hand, the KEA13 procedure yields a factor of safety of 0.93, resulting in a correct prediction of liquefaction triggering and an E_i of 0. With a Vs1-SW of 198 m/s, this site plots in the region where significant differences exist between the two Vs liquefaction evaluation procedures (Fig. 3). When using the Vs-SW profile, results from this site indicate that the KEA13 procedure is more correct. However, for the Vs-CPT profile, the average Vs1 for the critical layer is 135 m/s (63 m/s less than the Vs-SW value). Thus, both the A&S00 and KEA13 procedures result in false-positive predictions of liquefaction triggering at the site for the Darfield earthquake, with factors of safety of 0.50 and 0.62, respectively. These mispredictions result in E_i values of 0.034 and 0.028, respectively, for the A&S00 and KEA13 procedures. However, for the Christchurch earthquake, both the A&S00 and KEA13 procedures result in predictions that match the observed performance of liquefaction at the site, with factors of safety of 0.34 and 0.36, respectively, when using the Vs-CPT profile. Hence, the E_i values are equal to zero for both methods of analysis. For comparison, Green et al. (2014) showed that the Idriss and Boulanger (2008) The CPT liquefaction triggering procedure correctly predicts the observed performance of the site during both the Darfield and Christchurch earthquakes.

Discussion of Entire Data Set

The total E_I values for each Vs-based liquefaction evaluation procedure and each approach for obtaining Vs profiles (i.e., Vs-SW and Vs-CPT) are tabulated in Table 2. Based on these values,

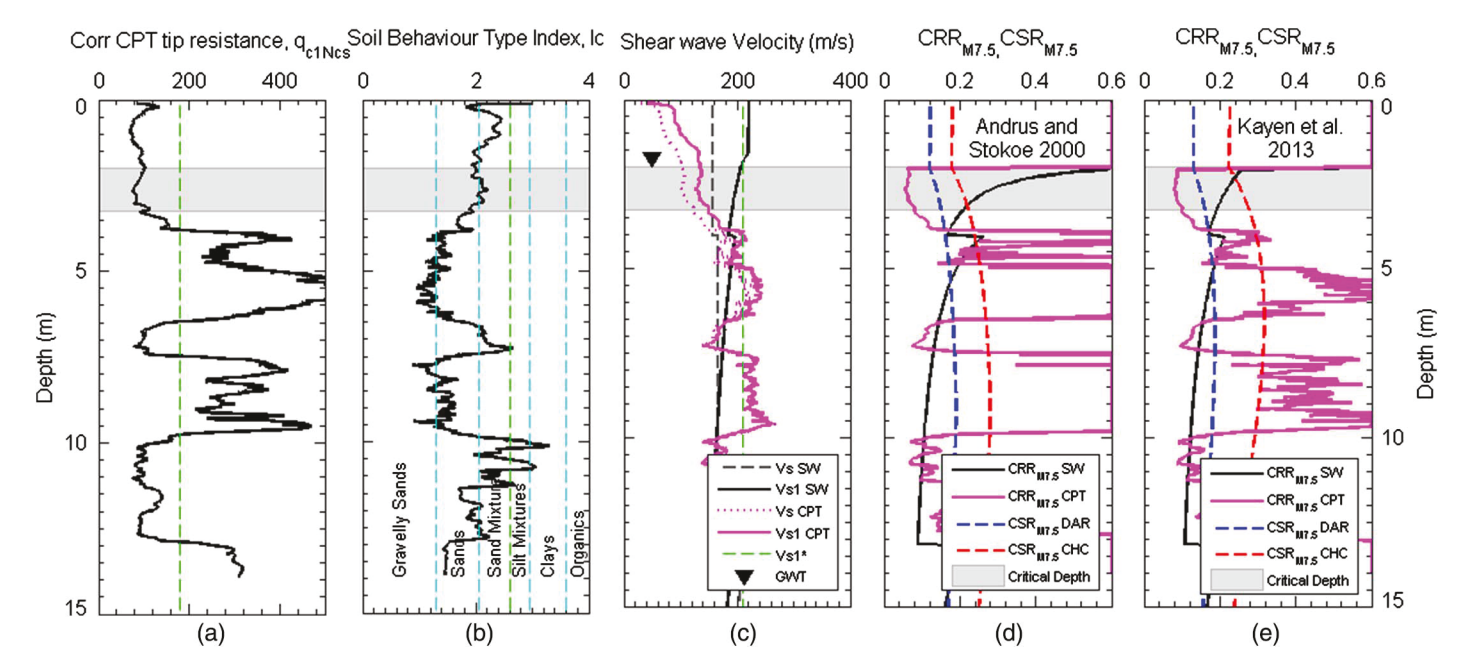


Fig. 5. (a) Corrected CPT tip resistance (q_{c1Ncs}) ; (b) soil behavior-type index (I_c) ; (c) raw and corrected Vs for SW and CPT (Vs and Vs1); (d) cyclic resistance ratio (CRR_{M7.5}) for SW and CPT; (e) cyclic stress ratio (CSR_{M7.5}) and Darfield and Christchurch earthquakes for Site 24: Z4-4; Vs1 shown is from A&S00 relationship

Table 2. Average E_I across All Sites for the Two Vs-Based Liquefaction Evaluation Procedures and Vs-SW and Vs-CPT Profiles

	E_I						
Parameter	A&S00 Vs-SW	KEA13 Vs-SW	A&S00 Vs-CPT	KEA13 Vs-CPT			
Darfield earthquake	0.094	0.068	0.263	0.242			
Christchurch earthquake	0.309	0.121	0.076	0.083			
Total for all sites	0.403	0.189	0.339	0.325			
Total for sites with Vs1 < 180 m/s	0.183	0.166	0.339	0.325			
Total for sites with $Vs1 > 180 \text{ m/s}$	0.220	0.023	0.000	0.000			

the following general conclusions can be drawn: (1) the KEA13 procedure generally results in lower E_I values than the A&S00 procedure and (2) the Vs-SW profiles result in lower E_I values for the Darfield earthquake, whereas the Vs-CPT profiles result in lower E_I values for the Christchurch earthquake. However, these general conclusions deserve additional scrutiny/explanation.

When considering case histories subjected to both moderate PGA values (Darfield earthquake) and high PGA values (Christchurch earthquake), it is clear that the KEA13 procedure, when coupled with the Vs-SW profiles, far outperforms the other combinations of analysis methods and Vs profiles, with a total E_I value of 0.189. The A&S00 procedure, when coupled with the Vs-SW profiles, results in the highest total E_I value of 0.408. More than one quarter of this high E_I value resulted from the falsenegative liquefaction case history associated with Site 24 for the Christchurch earthquake (as discussed in detail previously). However, three other false-negative predictions associated with the Christchurch earthquake also contributed significantly. These false-negative case history data points are shown as closed circles below the A&S liquefaction triggering curves in Fig. 3(a). In comparison, the KEA13 curve with a 15% probability of exceedance (i.e., the deterministic curve) only resulted in two false-negative case history data points, which plot closer to the line [Fig. 3(b)]. When using the Vs-SW profiles, both triggering relationships suffered from seven total false-positives out of the 12 no-liquefaction case histories. The no-liquefaction errors for the two relationships were virtually the same (Table 2). In other words, the higher E_I values associated with the A&S00 procedure are primarily driven by a few false-negative case histories that have Vs1 > 180 m/s in the critical layer. Because the A&S00 procedure incorporates a limiting upper-bound value of Vs1 for liquefaction (i.e., Vs1*), which ranges 200–215 m/s depending on fines content, the CRR curves are very steep and yield high factors of safety at high Vs1 values. By comparison, the KEA13 relationship is not nearly as steep at high Vs1 values. Based on these results, the KEA13 relationship for liquefaction triggering evaluations is recommend if Vs1 exceeds 180 m/s.

If the general performance of the Vs-CPT profiles compared with the Vs-SW profiles for all case histories shown in Figs. 3(a–d) are examined for both A&S00 and KEA13 relationships, the Vs-CPT data points have systematically lower Vs1 values than the Vs-SW data points, resulting in an apparent leftward shift (lower Vs1) of the Vs-CPT data points relative to the liquefaction triggering curves. The end result is that the Vs-CPT profiles result in more false-positive predictions of liquefaction. In fact, considering the no-liquefaction case histories from both earthquakes, the Vs-CPT profiles only yielded a correct prediction of no-liquefaction at 1 out of 12 sites when using the A&S00 procedure and 0 out of 12 sites when using the KEA13 procedure. However, the Vs-CPT profiles resulted in no false-negative predictions using either procedure.

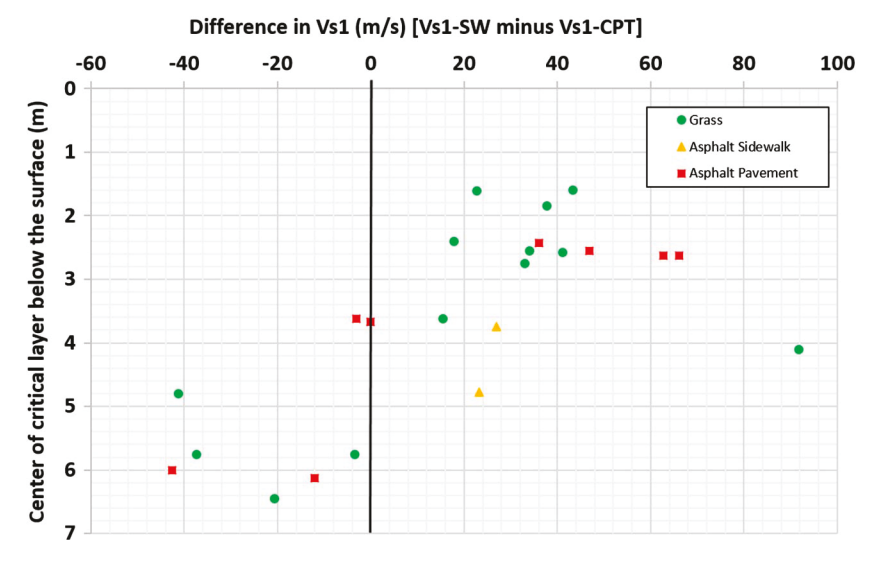


Fig. 6. Difference in overburden-corrected shear-wave velocity (Vs1) within critical layer between Vs1-SW and Vs1-CPT as a function of depth of center of critical layer (KEA13 Vs1 values used for the comparison); labeled according to surface conditions at testing site

As mentioned earlier, a bias between Vs-SW and Vs-CPT [when using the McGann et al. (2015a) correlation] was documented by McGann et al. (2015b), with the Vs correlated from CPT tip resistance being systematically less than the Vs obtained from surface wave testing over the top 6 m. The Vs-CPT profiles in the present study also seem to yield Vs that is substantially lower than the Vs-SW profiles, as evidenced by the higher number of falsepositive liquefaction predictions based on Vs-CPT. To investigate this bias further, the differences between the average Vs1-SW and the average Vs1-CPT in the critical layer for each case history are plotted as a function of the average depth of the critical layer in Fig. 6. From this plot, it is clear that the McGann et al. (2015a) Vs-CPT correlation systematically yields lower Vs1 values than those obtained from surface wave testing over the top 4–5 m. However, the Vs1-CPT values are generally greater than the Vs1-SW values at depths greater than 5 m. Several potential reasons for this bias are examined next.

First, it is always preferred to directly measure a quantity rather than to obtain it indirectly via correlation. Hence, the Vs-SW profiles should be favored above the correlated Vs-CPT profiles. However, it could be argued that obtaining Vs from surface wave testing is not a direct measurement, particularly given the potential uncertainties associated with surface wave inversion. The authors have investigated these general uncertainties in a number of recent papers (e.g., Cox and Teague 2016; Teague and Cox 2016; Griffiths et al. 2016a, b; Garofalo et al. 2016a, b; Teague et al. 2015; Foti et al. 2015; Cox et al. 2014; Wood et al. 2014). These papers illustrate that Vs derived from surface wave testing is least uncertain near the surface, that the use of a priori information to constrain the inversion helps to greatly reduce Vs uncertainty, and that in some cases Vs profiles derived from surface wave testing actually suffer from less uncertainty than Vs profiles derived from various borehole methods (i.e., downhole, cross hole, suspension logging) applied at the same site (Garofalo et al. 2016a). The specific details of the inversion procedure used in this study, and the potential pitfalls involved in this procedure, have been detailed. One such pitfall is associated with potentially poor resolution of the near-surface Vs-SW profiles at some sites due to testing through stiff asphalt surface layers. The effect of testing through asphalt is investigated by further subdividing the case history data points in Fig. 6 ground surface conditions at the test sites (i.e., grass, thin asphalt sidewalk,

asphalt pavement). No visible trend in the data is observed related to the type of material on which the surface wave testing was conducted. Hence, it is not believed that the near-surface Vs-SW values were biased too high by testing through asphalt in some cases.

In general, the first two authors have occasionally observed errors associated with Vs measured with SCPT in the top several meters of the subsurface. These errors are due to unknown wave propagation paths coupled with triggering inconsistencies that have a strong impact on results obtained using the pseudo-interval method of SCPT data analysis. Thus, it is possible that some of the SCPT Vs profiles used in the McGann et al. (2015a) correlation were biased to low velocities in the near surface. Additionally, several of the authors recently measured 30 Vs profiles at sites in Christchurch using the direct-push cross hole method (DPCH). SCPT testing was also independently conducted by a single contractor at each of these sites. Although not yet published, some of the authors have observed that the Vs profiles measured by SCPT were significantly lower than the Vs profiles measured by DPCH over the top several meters at many of these sites. For these reasons, the authors believe the Vs profiles correlated from CPT tip resistance may be artificially low over the top several meters, resulting in more false-positive predictions of liquefaction triggering than the Vs-SW profiles, as noted earlier.

Although the main focus of this paper is on comparing methods used to obtain Vs and on results obtained from Vs-based liquefaction triggering procedures, with particular attention given to the critical layers used for liquefaction triggering evaluations, at some sites (including the two example sites discussed in detail) large increases in CPT tip resistance are observed below the critical layer. However, these large increases are generally not mirrored by proportionally large increases in the Vs-SW measurements. This may be due to the fact that CPT measurements taken in gravelly soils are often unreliable because, when the cone directly encounters a gravel particle, high tip resistances are often measured which are not representative of the overall density of the stratum. Accordingly, the CPT q_c values and Vs-CPT values should not be blindly used when gravel layers are present. Furthermore, one would not expect a direct, linear relationship between small-strain stiffness (i.e., Vs) and large-strain strength/density (i.e., CPT tip resistance). These two parameters are sensitive to different soil properties and are not perfectly correlated with one another.

Specific to liquefaction triggering evaluations, the CRR curves for both A&S00 and KEA13 were developed from a significant number of case histories for which Vs was obtained using surface wave methods. As a result, any potential bias in the underprediction or overprediction of Vs from surface wave measurements relative to Vs-CPT estimates is inherent in the CRR curves. Accordingly, although it is difficult to state whether Vs-SW or Vs-CPT is more accurate, it can be stated that Vs-SW is more appropriate for evaluating liquefaction potential using existing Vs-based CRR relationships (e.g., A&S00 and KEA13) because of the compensating bias principle. That is, the Vs liquefaction triggering relationships were developed using many Vs profiles obtained from surface wave testing. Therefore, any systematic bias associated with Vs obtained from surface wave testing would be directly accounted for in the liquefaction triggering relationship. However, this would not be true for the Vs values determined using the McGann et al. (2015a) Vs-CPT correlation. The fact that the Vs-CPT profiles yield lower E_I values than the Vs-SW profiles for the case history data points associated with the Christchurch earthquake (Table 2) seems to be primarily driven by the relative numbers of liquefaction and no-liquefaction case history data points, with the majority of the case histories associated with the higher PGA values of the Christchurch earthquake being liquefaction cases. The Christchurch case history data are heavily weighted with liquefaction cases (as opposed to no-liquefaction cases). This fact, combined with Vs values developed using the Vs-CPT correlation that seem to be low relative to the Vs-SW values, results in lower E_I values for this particular data set. However, it is important to understand the underlying factors driving these lower E_I values.

It is interesting to compare the best total E_I value obtained in this study (i.e., $E_I = 0.189$ for the Vs-SW profiles coupled with the KEA13 procedure) with those published in Green et al. (2014) using three CPT-based liquefaction triggering relationships [i.e., Robertson and Wride (1998), R&W98; Moss et al. (2006), MEA06; and Idriss and Boulanger (2008), I&B08]. The CPT-based R&W98 procedure resulted in a total $E_I = 0.360$, the MEA06 procedure resulted in a total $E_I = 0.415$, and the I&B08 procedure resulted in a total $E_I = 0.08$. Thus, only the I&B08 CPT-based triggering relationship had a lower total error when considering the entire data set. More specifically, the KEA13 Vs and I&B08 CPT relationships both had a number of false-positives (seven for KEA13 and three for I&B08) and a number of false-negatives (two for KEA13 and four for I&B08). These differences indicate that the KEA13 Vs procedure may be slightly more conservative than the I&B08 CPT procedure, at least for this data set. Other data sets may yield different results. These comparisons of total E_I values were based on direct comparisons between the 23 sites (46 case histories) used in this study. Hence, 2 sites (4 case histories) were removed from the original Green et al. (2014) data set prior to calculating new E_I values to ensure an accurate comparison.

Summary and Conclusions

The 2010–2011 Canterbury earthquake sequence provides an unprecedented opportunity to add a number of well-documented case histories to the Vs-based liquefaction triggering database. This paper examined 46 Vs-based liquefaction case histories out of the original 50 CPT-based liquefaction case histories published by Green et al. (2014). The Vs profiles at each site were developed using (1) surface wave measurements made by the authors at each site and (2) a Christchurch-specific Vs-CPT correlation developed by McGann et al. (2015a). The surface wave-derived Vs profiles relied on the CPT results from Green et al. (2014) to determine

the critical layer and soil type, as should be done when conducting liquefaction analysis using Vs measurements. The case histories have been used to evaluate the two most common Vs-based simplified liquefaction triggering procedures (i.e., Andrus and Stokoe 2000; Kayen et al. 2013). An error index has been used to quantify the overall relative performance of these two procedures. The results indicate that the Kayen et al. (2013) procedure, using the 15% probability of liquefaction curve, provides more accurate predictions than the Andrus and Stokoe (2000) deterministic procedure for sites with Vs1 in the critical layer greater than 180 m/s. However, the procedures are essentially equivalent for sites with Vs1 < 180 m/s in the critical layer. Additionally, total error values obtained using Vs-SW profiles in conjunction with the Kayen et al. (2013) Vs-based procedure are lower than those obtained using two other CPT-based triggering procedures but higher than the total error values obtained using the Idriss and Boulanger (2008) CPTbased procedure. Scrutiny of the differences between the Kayen et al. (2013) and Idriss and Boulanger (2008) procedures shows that the Kayen et al. (2013) procedure results in four more false-positive predictions and two fewer false-negative predictions. Thus, it proves to be slightly more conservative but less accurate than the Idriss and Boulanger (2008) CPT-based procedure for the 46 case histories examined. Although the authors expect the trends in error values to remain consistent for other data sets, it is possible that they will not be mirrored in other case history databases.

Acknowledgments

The authors gratefully acknowledge the Canterbury Geotechnical Database and the New Zealand GeoNet project and its sponsors, the Earthquake Commission (EQC), GNS Science, and LINZ, for providing some of the data used in this study. Also, the authors are grateful to Mr. Josh Zupan and Dr. Jonathan Bray, who oversaw the performance of some of the CPT soundings presented in this study. The primary support for the U.S. authors was provided by National Science Foundation (NSF) Grants CMMI-1030564, CMMI-1407428, CMMI-1137977, CMMI-1435494, CMMI-1724575, and CMMI-1724915. Primary support for L. Wotherspoon was provided by the EQC. Any opinions, findings, conclusions, or recommendations expressed in this material are those of the authors and do not necessarily reflect the views of the National Science Foundation or the other funding agencies.

Supplemental Data

Case history summaries (Tables S1–S51 and Figs. S1–S96) and CRR plots (Figs. S92–S95) are available online in the ASCE Library (www.ascelibrary.org).

References

Andrus, R. D., and Stokoe, K. H., II. (2000). "Liquefaction resistance of soils from shear-wave velocity." *J. Geotech. Geoenviron. Eng.*, 10.1061 /(ASCE)1090-0241(2000)126:11(1015), 1015–1025.

Bradley, B. A. (2012a). "Ground motions observed in the Darfield and Christchurch earthquakes and the importance of local site response effects." N. Z. J. Geol. Geophys., 55(3), 279–286.

Bradley, B. A. (2012b). "Strong ground motion characteristics observed in the 4 September 2010 Darfield, New Zealand earthquake." *Soil Dyn. Earthquake Eng.*, 42, 32–46.

Bradley, B. A. (2014). "Site-specific and spatially distributed estimation of ground motion intensity in the 2010–2011 Canterbury earthquakes." Soil Dyn. Earthquake Eng., 61–62(1), 83–91.

- Bradley, B. A., and Cubrinovski, M. (2011). "Near-source strong ground motions observed in the 22 February 2011 Christchurch earthquake." Seismol. Res. Lett., 82(6), 853–865.
- Bradley, B. A., Quigley, M., Van Dissen, R., and Litchfield, N. J. (2014). "Ground motion and seismic rupture aspects of the 2010-2011 Canterbury earthquake sequence." *Earthquake Spectra*, 30(1), 1–15.
- Bray, J., Cubrinovski, M., Bradley, B. A., and Taylor, M. (2014). "Liquefaction effects on buildings in the central business district of Christchurch." *Earthquake Spectra*, 30(1), 85–109.
- Brown, L. J., Beetham, R. D., Paterson, B. R., and Weeber, J. H. (1995). "Geology of Christchurch, New Zealand." *Environ. Eng. Geosci.*, I(4), 427–488.
- Buchanan, A. H., Bull, D., Dhakal, R. P., MacRae, G., and Pampanin, S. (2011). "Base-isolation and damage-resistant technologies for improved seismic performance of buildings." (http://canterbury.royalcommission.govt.nz/Technical-Reports) (Aug., 2011).
- Cousins, J., and McVerry, G. (2010). "Overview of strong motion data from the Darfield earthquake." Bull. N. Z. Soc. Earthquake Eng., 43(4), 222–227.
- Cox, B., and Wood, C. (2011). "Surface wave benchmarking exercise: Methodologies, results and uncertainties." GeoRisk 2011: Geotechnical risk assessment and management, C. H. Juang, et al., eds., ASCE, Reston, VA, 224.
- Cox, B., Wood, C., Ellis, T., and Teague, D. (2014). "Synthesis of the UTexas1 surface wave dataset blind-analysis study: Inter-analyst dispersion and shear wave velocity uncertainty." Proc., Geo-Congress 2014: Geo-Characterization and Modeling for Sustainability, ASCE, Reston, VA, 850–859.
- Cox, B. R., and Beekman, A. N. (2011). "Intramethod variability in ReMi dispersion measurements and Vs estimates at shallow bedrock sites." *J. Geotech. Geoenviron. Eng.*, 10.1061/(ASCE)GT.1943-5606.0000436, 354–362.
- Cox, B. R., and Teague, D. P. (2016). "Layering ratios: A systematic approach to the inversion of surface wave data in the absence of a-priori information." *Geophys. J. Int.*, 207(1), 422–438.
- Cubrinovski, M., et al. (2010). "Geotechnical reconnaissance of the 2010 Darfield (Canterbury) earthquake." Bull. N. Z. Soc. Earthquake Eng., 43(4), 243–320.
- Cubrinovski, M., et al. (2011). "Geotechnical aspects of the 22 February 2011 Christchurch earthquake." *Bull. N. Z. Soc. Earthquake Eng.*, 44(4), 205–226.
- El-Sekelly, W., Abdoun, T., and Dobry, R. (2015). "Liquefaction resistance of a silty sand deposit subjected to preshaking followed by extensive liquefaction." J. Geotech. Geoenviron. Eng., 10.1061/(ASCE)GT .1943-5606.0001444, 04015101.
- Forsyth, P., Barrell, D., and Jongens, R. (2008). *Geology of the Christ-church area, Institute of Geological and Nuclear Sciences Geological Map 16*, GNS Science, Lower Hutt, New Zealand, 67.
- Foti, S., et al. (2015). "Uncertainties in Vs profiles from geophysical tests and their influence on seismic ground response analyses: Results from the InterPACIFIC blind test." *Proc.*, 6th Int. Conf. on Earthquake Geotechnical Engineering, International Society for Soil Mechanics and Geotechnical Engineering, London.
- Garofalo, F., et al. (2016a). "InterPACIFIC project: Comparison of invasive and non-invasive methods for seismic site characterization. I: Intracomparison of surface wave methods." Soil Dyn. Earthquake Eng., 82(1), 222–240.
- Garofalo, F., et al. (2016b). "InterPACIFIC project: Comparison of invasive and non-invasive methods for seismic site characterization. II: Intercomparison between surface wave and borehole methods." *Soil Dyn. Earthquake Eng.*, 82(1), 241–254.
- Green, R. A., et al. (2011). "Performance of levees (stopbanks) during the 4 September Mw7.1 Darfield and 22 February 2011 Mw6.2 Christchurch, New Zealand, earthquakes." Seismol. Res. Lett., 82(6), 939–949.
- Green, R. A., et al. (2014). "Select liquefaction case histories from the 2010–2011 Canterbury earthquake sequence." *Earthquake Spectra*, 30(1), 131–153.
- Green, R. A., Obermeier, S. F., and Olson, S. M. (2005). "Engineering geologic and geotechnical analysis of paleoseismic shaking using liquefaction effects: Field examples." *Eng. Geol.*, 76(3), 263–293.

- Green, R. A., and Olson, S. M. (2015). "Interpretation of liquefaction field case histories for use in developing liquefaction triggering curves." *Proc.*, 6th Int. Conf. on Earthquake Geotechnical Engineering (61CEGE), International Society for Soil Mechanics and Geotechnical Engineering, London.
- Griffiths, S. C., Cox, B. R., Rathje, E. M., and Teague, D. P. (2016a). "Mapping dispersion misfit and uncertainty in Vs profiles to variability in site response estimates." *J. Geotech. Geoenviron. Eng.*, 10.1061 /(ASCE)GT.1943-5606.0001553, 04016062.
- Griffiths, S. C., Cox, B. R., Rathje, E. M., and Teague, D. P. (2016b).
 "Surface wave dispersion approach for evaluating statistical models that account for shear-wave velocity uncertainty." *J. Geotech. Geoenviron. Eng.*, 10.1061/(ASCE)GT.1943-5606.0001552, 04016061.
- Idriss, I. M., and Boulanger, R. W. (2008). *Soil liquefaction during earth-quakes*, Earthquake Engineering Research Institute, Oakland, CA.
- Joh, S. H. (1996). "Advances in interpretation and analysis techniques for spectral-analysis-of-surface-waves (SASW) measurements." Ph.D. dissertation, Dept. of Civil, Architectural, and Environmental Engineering, Univ. of Texas, Austin, TX.
- Kayen, R., et al. (2013). "Shear-wave velocity-based probabilistic and deterministic assessment of seismic soil liquefaction potential." J. Geotech. Geoenviron. Eng., 10.1061/(ASCE)GT.1943-5606.0000743, 407–419.
- Louie, J. N. (2001). "Faster, better shear wave velocity to 100 meters depth from refraction microtremor arrays." *Bull. Seismol. Soc. Am.*, 91(2), 347–364.
- McGann, C. R., Bradley, B. A., Taylor, M., Wotherspoon, L. M., and Cubrinovski, M. (2015a). "Development of an empirical correlation for predicting shear wave velocity of Christchurch soils from cone penetration test data." Soil Dyn. Earthquake Eng., 75, 66–75.
- McGann, C. R., Bradley, B. A., Wotherspoon, L. M., and Cox, B. R. (2015b).
 "Comparison of a Christchurch-specific CPT-VS correlation and Vs derived from surface wave analysis for strong motion station velocity characterisation." Bull. N. Z. Soc. Earthquake Eng., 48(2), 81–91.
- Moss, R. E. S., Seed, R. B., Kayen, R. E., Stewart, J. P., Der Kiureghian, A., and Cetin, K. O. (2006). "CPT-based probabilistic and deterministic assessment of in situ seismic soil liquefaction potential." *J. Geotech. Geoenviron. Eng.*, 132, 1032–1051.
- Olson, S. M., Green, R. A., and Obermeier, S. F. (2005). "Engineering geologic and geotechnical analysis of paleoseismic shaking using lique-faction effects: A major updating." *Eng. Geol.*, 76(3–4), 235–261.
- Quigley, M. C., Bastin, S., and Bradley, B. A. (2013). "Recurrent liquefaction in Christchurch, New Zealand, during the Canterbury earthquake sequence." *Geology*, 41(4), 419–422.
- Robertson, P. (2015). "Comparing CPT and Vs liquefaction triggering methods." *J. Geotech. Geoenviron. Eng.*, 10.1061/(ASCE)GT.1943 -5606.0001338, 04015037.
- Robertson, P. K., and Wride, C. E. (1998). "Evaluating cyclic liquefaction potential using the cone penetration test." *Can. Geotech. J.*, 35(3), 442–459.
- Robinson, K., Cubrinovski, M., and Bradley, B. A. (2012). "Comparison of actual and predicted measurements of liquefaction-induced lateral displacements from the 2010 Darfield and 2011 Christchurch earthquakes." *Proc.*, 2012 Conf. of the New Zealand Society for Earthquake Engineering (NZSEE 2012), New Zealand Society for Earthquake Engineering, Wellington, New Zealand, 1–8.
- Schneider, J. A., and Moss, R. E. S. (2011). "Linking cyclic stress and cyclic strain based methods for assessment of cyclic liquefaction triggering in sands." Géotech. Lett., 1(2), 31–36.
- SeisOpt ReMi [Computer software]. Optim, Reno, NV.
- Stokoe, K. H., Wright, S. G., Bay, J. A., and Roesset, J. M. (1994). "Characterization of geotechnical sites by SASW method." *Proc.*, 13th Int. Conf. on Soil Mechanics and Foundation Engineering, CRC Press, Boca Raton, FL, 923–930.
- Teague, D. P., and Cox, B. R. (2016). "Site response implications associated with using non-unique Vs profiles from surface wave inversion in comparison with other commonly used methods of accounting for Vs uncertainty." Soil Dyn. Earthquake Eng., 91, 87–103.
- Teague, D. P., Cox, B. R., Bradley, B. A., and Wotherspoon, L. M. (2015).
 "Development of realistic Vs profiles in Christchurch, New Zealand via active and ambient surface wave data: Methodologies for inversion in

- complex interbedded geology." *Proc., 6th Int. Conf. on Earthquake Geotechnical Engineering*, International Society for Soil Mechanics and Geotechnical Engineering, London.
- Wood, C., Ellis, T., Teague, D., and Cox, B. (2014). "Analyst I: Comprehensive analysis of the UTexas1 surface wave dataset." 2014 Geo-Congress: Geo-Characterization and Modeling for Sustainability, ASCE, Reston, VA, 820–829.
- Wood, C. M., Cox, B. R., Wotherspoon, L. M., and Green, R. A. (2011).
 "Dynamic site characterization of Christchurch strong motion stations."
 Bull. N. Z. Soc. Earthquake Eng., 44(4), 195–204.
- Wood, C. M., Wotherspoon, L. M., and Cox, B. R. (2015). "Influence of a-priori subsurface layering data on the development of realistic shear wave velocity profiles from surface wave inversion." *Proc.*, 6th Int. Conf. on Earthquake Geotechnical Engineering, International Society for Soil Mechanics and Geotechnical Engineering, London.
- Wotherspoon, L. M., Orense, R. O., Bradley, B. A., Cox, B. R., Wood, C. M., and Green, R. A. (2015). "Soil profile characterisation of

- Christchurch central business district strong motion stations." *Bull. N. Z. Soc. Earthquake Eng.*, 48(3), 147–157.
- Wotherspoon, L. M., Orense, R. P., Bradley, B. A., Cox, B. R., Wood, C. M., and Green, R. A. (2013). "Soil profile characterisation of Christchurch strong motion stations." *EQC Biennial Grant Rep. 12/629*, New Zealand Society for Earthquake Engineering, Wellington, New Zealand.
- Wotherspoon, L. M., Pender, M. J., and Orense, R. P. (2012). "Relationship between observed liquefaction at Kaiapoi following the 2010 Darfield earthquake and former channels of the Waimakariri River." *Eng. Geol.*, 125(1), 45–55.
- Yoon, S., and Rix, G. J. (2009). "Near-field effects on array-based surface wave methods with active sources." J. Geotech. Geoenviron. Eng., 10.1061/(ASCE)1090-0241(2009)135:3(399), 399–406.
- Zywicki, D. J. (1999). "Advanced signal processing methods applied to engineering analysis of seismic surface waves." Ph.D. dissertation, School of Civil and Environmental Engineering, Georgia Institute of Technology, Atlanta.